Comparing pertinent effects of antiferromagnetic fluctuations in the two- and three-dimensional Hubbard model

A. A. Katanin,[1,2] A. Toschi,[1,3] and K. Held[3]
[1]*Max-Planck-Institut für Festkörperforschung, 70569 Stuttgart, Germany*
[2]*Institute of Metal Physics, 620044 Ekaterinburg, Russia*
[3]*Institute of Solid State Physics, Vienna University of Technology, 1040 Vienna, Austria*
(Received 27 April 2009; published 5 August 2009)

We use the dynamical vertex approximation (DΓA) with a Moriyaesque λ correction for studying the impact of antiferromagnetic fluctuations on the spectral function of the Hubbard model in two and three dimensions. Our results show the suppression of the quasiparticle weight in three dimensions and dramatically stronger impact of spin fluctuations in two dimensions where the pseudogap is formed at low enough temperatures. Even in the presence of the Hubbard subbands, the origin of the pseudogap at weak-to-intermediate coupling is in the splitting of the quasiparticle peak. At stronger coupling (closer to the insulating phase) the splitting of Hubbard subbands is expected instead. The **k** dependence of the self-energy appears to be also much more pronounced in two dimensions as can be observed in the **k**-resolved DΓA spectra, experimentally accessible by angular resolved photoemission spectroscopy in layered correlated systems.

DOI: 10.1103/PhysRevB.80.075104 PACS number(s): 71.27.+a, 71.10.Fd

I. INTRODUCTION

Since its formulation,[1] the Hubbard model served as a minimal model for electronic correlations. Due to the complexity of electronic correlations, solving this model is however only possible in dimension $d=1$ (exactly via the Bethe Ansatz[2]) and in the limit $d=\infty$ (Refs. 3–5) (where the mapping[4] onto an Anderson impurity model allows for an accurate numerical solution[5,6]). Of physical interest are however strongly correlated systems in $d=3$, for modeling the Mott-Hubbard transition[7] and (anti)ferromagnetism,[1,8,9] and in $d=2$ for describing the cuprates,[10] where the role of the antiferromagnetic fluctuations in developing pseudogap structures and superconductivity are at the center of attention.

The aim of this paper is to study the difference between the effect of antiferromagnetic fluctuations on the electronic properties in $d=2$ and $d=3$. For weak coupling (small Coulomb interaction U), the perturbation theory, and its extensions, e.g., the fluctuation-exchange approximation (FLEX),[11] the two-particle self-consistent (TPSC) approximation,[12] and the functional renormalization group[13] are suitable methods for this purpose. In $d=3$ antiferromagnetic fluctuations produce only quantitative changes of electronic spectrum, although the particle-hole excitations enhance the quasiparticle scattering rate when the temperature T is approaching the Néel temperature. In $d=2$ there are divergences in the self-energy diagrams and the above-mentioned approximations predict pseudogap structures in the self-energy in the weak-coupling regime.[14–16] These techniques are however not applicable at stronger coupling since they do not describe strong quasiparticle renormalization due to the Mott physics.

Since we are interested in intermediate-to-strong electronic correlations, we need to take a different approach. Starting point is the by-now widely employed dynamical mean-field theory (DMFT).[3–5] This method becomes exact[3] for $d\to\infty$, and yields a major part of the electronic correlations, i.e., the local correlations. However, any nonlocal correlations are neglected and hence DMFT does not differentiate between the Hubbard model in two and three dimensions. More precisely, only differences stemming from different shapes of the density of states (DOS) are taken into account, not those resulting, e.g., from antiferromagnetic correlations since these correlations are by nature nonlocal.

Hitherto, the focus of DMFT extensions has been on *short-range* correlations within a (finite) cluster instead of the single DMFT impurity site. These cluster extensions of DMFT (Ref. 17) have been used for describing pseudogaps and superconductivity in the two-dimensional (2D) Hubbard model. Due to numerical limitations, the inclusion of important *long-range* correlations and the application of this method in three dimensions or realistic multiorbital calculations is however not possible, except for very small clusters with $\mathcal{O}(2–4)$ sites. Also the $1/d$ expansion of DMFT (Ref. 18) is restricted to *short-range* correlations, as is a recent perturbative extension.[19]

Hence, for including *long-range* correlations, the focus of the methodological development has shifted recently to diagrammatic extensions of DMFT such as the dynamical vertex approximation (DΓA) (Refs. 20–23) and the dual fermion approach by Rubtsov *et al.*[24] Even before, Kuchinskii *et al.*[25] combined the local DMFT self-energy with the nonlocal contributions to self-energy of the spin-fermion model, and included long-range correlations this way. Their procedure, however, does not rely on a rigorous diagrammatic derivation.

To include long-range fluctuations in a diagrammatic way DΓA considers the local vertex instead of the bare interaction. It includes DMFT but also long-range correlations beyond. Our understanding of the physics associated with such long-range correlation is typically based on ladder diagrams, which are considered, e.g., by the above-mentioned TPSC and FLEX approximations. For example, the ladder diagrams in the particle-hole channel yield antiferromagnetic fluctuations in the paramagnetic phase (paramagnons) and (anti)fer-

romagnons in the ordered state. It is natural to suppose that the contribution of the corresponding fluctuations in the intermediate coupling regime can be described by the same kind of diagrams albeit with the *renormalized* vertices. In DΓA the local (frequency dependent) vertex is considered instead of the bare interaction. Therefore, this method reproduces the results of the weak-coupling approaches at small U but can treat spatial correlations also at intermediate coupling. Hence, DΓA is well suited for studying antiferromagnetic fluctuations in strongly correlated systems both for $d=2$ and $d=3$.

The paper is organized as follows: In Sec. II we reiterate the DΓA approach in a formulation with the three-point (instead of the four-point) vertex functions which allows for a connection to the spin-fermion model in Sec. III and for the analytical considerations on the DΓA self-energy in Sec. IV. In Sec. V, we introduce a Moriyaesque λ correction to the susceptibility to describe correctly the two-dimensional case. Results for three dimensions are presented in Sec. VI and compared to those in two dimensions in Sec. VII. Special emphasis to angular resolved spectra is given in Sec. VIII before we give a brief summary in Sec. IX.

II. DYNAMICAL VERTEX APPROXIMATION

Starting point of our considerations is the Hubbard model on a square or cubic lattice

$$H = -t\sum_{\langle ij\rangle\sigma} c^{\dagger}_{i\sigma}c_{j\sigma} + U\sum_{i} n_{i\uparrow}n_{i\downarrow}, \tag{1}$$

where t denotes the hopping amplitude between nearest neighbors, U is the Coulomb interaction, $c^{\dagger}_{i\sigma}(c_{i\sigma})$ creates (annihilates) an electron with spin σ on site i; $n_{i\sigma}=c^{\dagger}_{i\sigma}c_{i\sigma}$. In the following, we restrict ourselves to the paramagnetic phase with $n=1$ electrons/site at a finite temperature T.

The DΓA result for the self-energy of model (1) was derived in Ref. 20, see Eq. (16). For the purpose of the present paper this result for the self-energy can be written in the form

$$\Sigma_{\mathbf{k},\nu} = \frac{1}{2}Un + \frac{1}{2}TU\sum_{\nu'\nu''\omega,\mathbf{q}} [3\chi^{\nu'\nu''\omega}_{s,\mathbf{q}}\Gamma^{\nu''\nu\omega}_{s,\mathrm{ir}} - \chi^{\nu'\nu''\omega}_{c,\mathbf{q}}\Gamma^{\nu''\nu\omega}_{c,\mathrm{ir}} + \chi^{\nu'}_{0\mathbf{q}\omega}(\Gamma^{\nu\nu'\omega}_{c,\mathrm{loc}} - \Gamma^{\nu\nu'\omega}_{s,\mathrm{loc}})]\quad G_{\mathbf{k}+\mathbf{q},\nu+\omega}, \tag{2}$$

where the nonlocal spin (s) and charge (c) susceptibilities

$$\chi^{\nu\nu'\omega}_{s(c),\mathbf{q}} = [(\chi^{\nu'}_{0\mathbf{q}\omega})^{-1}\delta_{\nu\nu'} - \Gamma^{\nu\nu'\omega}_{s(c),\mathrm{ir}}]^{-1} \tag{3}$$

can be expressed in terms of the particle-hole bubble $\chi^{\nu'}_{0\mathbf{q}\omega} = -T\Sigma_{\mathbf{k}}G_{\mathbf{k},\nu'}G_{\mathbf{k}+\mathbf{q},\nu'+\omega}$, $G_{\mathbf{k},\nu}=[i\nu-\varepsilon_{\mathbf{k}}+\mu-\Sigma_{\mathrm{loc}}(\nu)]^{-1}$ is the Green's function, and $\Sigma_{\mathrm{loc}}(\nu)$ the local self-energy. The spin (charge) irreducible local vertices $\Gamma^{\nu\nu'\omega}_{s(c),\mathrm{ir}}$ are determined from the corresponding local problem.[20]

Result (2) accounts for the contribution of ladder diagrams to the self-energy in the two particle-hole channels. Following Edwards and Hertz[26] it is convenient to pick out parts of these ladders, which are separated by the bare on-site Coulomb interaction U. This is achieved by considering the quantities

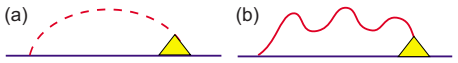

FIG. 1. (Color online) Graphical representation of the contribution of (a) bare Coulomb interaction and (b) spin (charge) fluctuations to the self-energy in the DΓA approach, Eq. (8). Solid lines correspond to the electronic Green's function $G_{\mathbf{k},\nu}$, dashed line to the bare Hubbard interaction U, wiggly lines—to the spin (charge) susceptibility $\chi^{s(c)}_{\mathbf{q},\omega}$; the triangle corresponds to the interaction vertex $\gamma^{\nu,\omega}_{s(c),\mathbf{q}}$.

$$\Phi^{\nu\nu'\omega}_{s(c),q} = [(\chi^{\nu'}_{0\mathbf{q}\omega})^{-1}\delta_{\nu\nu'} - \Gamma^{\nu\nu'\omega}_{s(c),\mathrm{ir}} \pm U]^{-1},$$

$$\phi^{s(c)}_{\mathbf{q},\omega} = \sum_{\nu\nu'} \Phi^{\nu\nu'\omega}_{s(c),\mathbf{q}}, \tag{4}$$

such that $\chi^{\nu\nu'\omega}_{s(c),\mathbf{q}} = \{[\Phi^{\nu\nu'\omega}_{s(c),q}]^{-1} \mp U\}^{-1}$ with the upper (lower) sign for the spin (charge) susceptibility. The nonlocal spin (charge) susceptibility is then given by

$$\chi^{s(c)}_{\mathbf{q}\omega} = \sum_{\nu\nu'} \chi^{\nu\nu'\omega}_{s(c),\mathbf{q}} = [(\phi^{s(c)}_{\mathbf{q},\omega})^{-1} \mp U]^{-1}, \tag{5}$$

and therefore $\phi^{s(c)}_{\mathbf{q},\omega}$ provided to be a particle-hole irreducible susceptibility in the spin (charge) channel. Introducing, similar to Ref. 26, the corresponding three-point vertex $\gamma^{\nu\omega}_{s(c),\mathbf{q}}$ of electron interaction with charge (spin) fluctuations,

$$\gamma^{\nu\omega}_{s(c),\mathbf{q}} = (\chi^{\nu}_{0\mathbf{q}\omega})^{-1}\sum_{\nu'} \Phi^{\nu\nu'\omega}_{s(c),\mathbf{q}}, \tag{6}$$

the irreducible susceptibility $\phi^{s(c)}_{\mathbf{q},\omega}$ can be represented as

$$\phi^{s(c)}_{\mathbf{q},\omega} = \sum_{\nu} \gamma^{\nu\omega}_{s(c),\mathbf{q}}\chi^{\nu}_{0\mathbf{q}\omega}. \tag{7}$$

In these notations, result (2) can then be rewritten identically as

$$\Sigma_{\mathbf{k},\nu} = \frac{1}{2}Un + \frac{1}{2}TU\sum_{\omega,\mathbf{q}}\Bigg[3\gamma^{\nu\omega}_{s,\mathbf{q}} - \gamma^{\nu\omega}_{c,\mathbf{q}} - 2 + 3U\gamma^{\nu\omega}_{s,\mathbf{q}}\chi^{s}_{\mathbf{q}\omega} + U\gamma^{\nu\omega}_{c,\mathbf{q}}\chi^{c}_{\mathbf{q}\omega} + \sum_{\nu'}\chi^{\nu'}_{0\mathbf{q}\omega}(\Gamma^{\nu\nu'\omega}_{c,\mathrm{loc}} - \Gamma^{\nu\nu'\omega}_{s,\mathrm{loc}})\Bigg]\ G_{\mathbf{k}+\mathbf{q},\nu+\omega}. \tag{8}$$

The first three terms in the square brackets correspond to the interaction of electrons via Hubbard on-site Coulomb interaction [without forming particle-hole bubbles, Fig. 1(a)], the next two terms correspond to electron interactions via charge and spin fluctuations [Fig. 1(b)], and the last term subtracts double counted local contribution.

III. RELATION TO SPIN-FERMION MODELS

The contributions of bare Coulomb interaction and charge (spin) fluctuations to self-energy (8) can be also obtained from the fermion-boson model with generating functional

$$Z = \int D[c^{\dagger}_{k\sigma}, c_{k\sigma}]D\mathbf{S}_{\mathbf{q},\omega}D\rho_{\mathbf{q},\omega}\exp\{-\mathcal{L}[\mathbf{S},\rho,c]\},$$

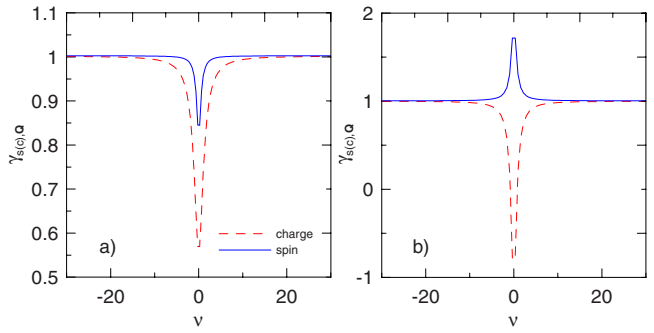

FIG. 2. (Color online) Frequency dependence of the spin and charge three-point vertex Eq. (6) at $U=1$, $\beta=1/T=15$ (left), and $U=2$, $\beta=10$ (right), $\omega=0$, at the antiferromagnetic wave vector $\mathbf{Q}=(\pi,\pi)$. All energies are in units of half the effective bandwidth $D\equiv 4t$.

$$\mathcal{L}[\mathbf{S},\rho,c] = \sum_{\mathbf{k},\nu,\sigma} (i\nu_n - \varepsilon_{\mathbf{k}}) c^{\dagger}_{k\sigma} c_{k\sigma} + U \sum_{\mathbf{q},\omega} (\rho_{q\omega}\rho_{-q,-\omega} + \mathbf{S}_{q\omega}\mathbf{S}_{-q,-\omega}) + U \sum_{\mathbf{k},\mathbf{q},\nu,\omega,\sigma,\sigma'} (\gamma^{\nu\omega}_{s,\mathbf{q}})^{1/2} c^{\dagger}_{\mathbf{k},\nu,\sigma} \boldsymbol{\sigma}_{\sigma\sigma'} c_{\mathbf{k}+\mathbf{q},\nu+\omega,\sigma'} \mathbf{S}_{\mathbf{q},\omega} + iU \sum_{\mathbf{k},\mathbf{q},\nu,\omega} (\gamma^{\nu\omega}_{c,\mathbf{q}})^{1/2} c^{\dagger}_{\mathbf{k},\nu,\sigma} c_{\mathbf{k}+\mathbf{q},\nu+\omega,\sigma} \rho_{\mathbf{q},\omega}, \tag{9}$$

where $\gamma^{\nu\omega}_{c(s),\mathbf{q}}$ is determined in the present approach according to the Eq. (6) and $\boldsymbol{\sigma}_{\sigma\sigma'}$ are the Pauli matrices. Model (9) is similar to that derived from the Hubbard model via Hubbard-Stratonovich transformation,[27] but it is explicitly spin symmetric and contains the nonlocal frequency dependent vertices $\gamma^{\nu\omega}_{c(s),\mathbf{q}}$, which account for the local—and short-range—nonlocal fluctuations.

Contrary to the earlier paramagnon theories[28] and the spin-fermion model,[29,30] where $\gamma^{\nu\omega}_{s,\mathbf{q}}=1$ and charge fluctuations are omitted ($\gamma^{\nu\omega}_{c,\mathbf{q}}=0$), we have $\gamma^{\nu\omega}_{s(c),\mathbf{q}}\neq 0$ and $\neq 1$. The frequency dependence of the vertices $\gamma^{\nu 0}_{s(c),\mathbf{Q}}$ calculated in the present approach for two dimensions with $\mathbf{Q}=(\pi,\pi)$ is shown in Fig. 2 (in the three-dimensional case we observe qualitatively similar behavior). One can see that both charge and spin vertices have a strong frequency dependence and approach unity only in the high-frequency limit. While in the weak-coupling regime $U=D\equiv 4t$ both vertices are suppressed at small frequencies [which is the consequence of the particle-particle (Kanamori) screening], closer to the DMFT Mott transition (at $U=2D\equiv 8t$) the spin vertex at small frequencies is *enhanced*. This behavior is similar to that observed in Ref. 20 for the three-frequency (four-point) vertex in the three-dimensional case.

Hence, the spin-fermion theory, which was heuristically added to the DMFT self-energy before, is included in a more systematic and consistent way in DΓA, which also accounts for the corrections to the electron-paramagnon vertex. The susceptibility $\chi^{s}_{q,\omega}$ which is determined phenomenologically in the spin-fermion model is obtained in our approach by dressing the bare propagator $1/U$ of charge and spin fields by particle-hole bubbles, which reproduces results (5) and (7) of the previous section.

Using model (9) one can also calculate the leading-order nonlocal correction to the three-point vertices due to fermion-boson interaction,

$$\tilde{\gamma}^{\nu\omega}_{s,\mathbf{k},\mathbf{q}} = \gamma^{\nu\omega}_{s,\mathbf{q}} + \frac{1}{2}TU \sum_{\omega_1,\mathbf{q}_1} \gamma^{\nu+\omega_1,\omega}_{s,\mathbf{q}} [2 - \gamma^{\nu\omega_1}_{s,\mathbf{q}_1} - \gamma^{\nu\omega_1}_{c,\mathbf{q}_1} - U\gamma^{\nu\omega_1}_{s,\mathbf{q}_1}\chi^{s}_{\mathbf{q}_1,\omega_1} + U\gamma^{\nu\omega_1}_{c,\mathbf{q}_1}\chi^{c}_{\mathbf{q}_1\omega_1}]\ G_{\mathbf{k}+\mathbf{q}_1,\nu+\omega_1} \times G_{\mathbf{k}+\mathbf{q}_1+\mathbf{q},\nu+\omega_1+\omega} - \mathrm{loc}, \tag{10}$$

$$\tilde{\gamma}^{\nu\omega}_{c,\mathbf{k},\mathbf{q}} = \gamma^{\nu\omega}_{s,\mathbf{q}} + \frac{1}{2}TU \sum_{\omega_1,\mathbf{q}_1} \gamma^{\nu+\omega_1,\omega}_{s,\mathbf{q}} [3\gamma^{\nu\omega_1}_{s,\mathbf{q}_1} - \gamma^{\nu\omega_1}_{c,\mathbf{q}_1} - 2 + 3U\gamma^{\nu\omega_1}_{s,\mathbf{q}_1}\chi^{s}_{\mathbf{q}_1,\omega_1} + U\gamma^{\nu\omega_1}_{c,\mathbf{q}_1}\chi^{c}_{\mathbf{q}_1\omega_1}]\ G_{\mathbf{k}+\mathbf{q}_1,\nu+\omega_1} \times G_{\mathbf{k}+\mathbf{q}_1+\mathbf{q},\nu+\omega_1+\omega} - \mathrm{loc}, \tag{11}$$

where loc stands for the subtraction of the local terms already included in $\gamma^{\nu\omega}_{s,\mathbf{q}}$. The nonlocal corrections to the self-energy and vertex can be then treated self-consistently by substituting them into Eq. (7). This provides an alternative simpler way of self-consistent treatment instead of the more complicated parquet approach discussed in Ref. 20. An even simpler way to go beyond a non-self-consistent treatment of the DΓA equations is considered in Sec. V.

IV. ANALYTIC APPROXIMATION FOR THE DΓA SELF-ENERGY

Similarly to the weak-coupling approach,[12] in the two-dimensional case the self-energy can be obtained approximately analytically. In this case the susceptibility $\chi^{s}_{\mathbf{q}\omega}$ is strongly enhanced at $\omega_n=0$ and $\mathbf{q}\approx\mathbf{Q}=(\pi,\pi)$, and can be represented in the form

$$\chi^{s}_{\mathbf{q}0} = \frac{A}{(\mathbf{q}-\mathbf{Q})^2 + \xi^{-2}}, \tag{12}$$

where $\xi^{-2}=A/(1-U\phi^{s}_{\mathbf{Q}0})$ with $A=(\nabla^2\phi^{s}_{\mathbf{q}0})_{\mathbf{q}=\mathbf{Q}}$ being the (squared) inverse spin-fluctuation correlation length. Since the corresponding momentum sum in Eq. (8) over $\mathbf{q}$ is logarithmically divergent at $\xi\to\infty$, we can approximately retain ourselves to only the zero bosonic Matsubara frequency term in the spin-fluctuation contribution and put $\mathbf{q}\approx\mathbf{Q}$ in all the factors except $\chi^{s}_{\mathbf{q}0}$ to obtain

$$\Sigma_{\mathbf{k},\nu} \simeq \Sigma_{\mathrm{loc}}(\nu) + \Delta^2 \gamma^{\nu,0}_{s,\mathbf{Q}} G_{\mathbf{k}+\mathbf{Q},\nu}, \tag{13}$$

where $\Delta^2=(3TU^2/2)\Sigma_{\mathbf{q}}\chi^{s}_{\mathbf{q},0}$.

To study the frequency dependence of self-energy (13) qualitatively, we first consider $\gamma^{\nu,0}_{s,\mathbf{Q}}=1$ and choose the local self-energy in the form (see, e.g., Ref. 31)

$$\Sigma_{\mathrm{loc}}(\nu) = (1-\kappa)(\Delta^2_{\mathrm{loc}}/4)/[\nu - \Delta^2_{\mathrm{loc}}\kappa/(4\nu)], \tag{14}$$

where $\Delta_{\mathrm{loc}}\simeq U$ is the size of the Hubbard gap and κ measures the relative weight of the quasiparticle peak (QP) with respect to the Hubbard subbands ($\kappa=0$ at the Mott transition and $\kappa=1$ for $U\to 0$). Equation (14) allows reproducing the

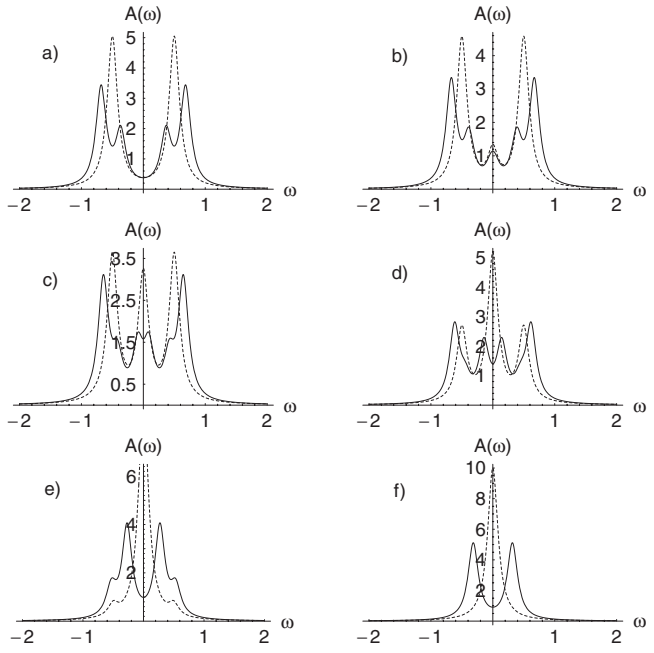

FIG. 3. The spectral functions in $d=2$ as obtained from the approximate self-energies including local [dashed lines, Eq. (14)] and nonlocal [solid lines, Eq. (13)] fluctuations for (a) $\kappa=0$, (b) 0.1, (c) 0.3, (d) 0.5, (e) 0.9, and (f) 1.0.

three-peak structure of the self-energy, observed in the numerical solution of the single-impurity Anderson model, supplemented by the DMFT self-consistent condition.

The evolution of the spectral properties calculated with self-energies (13) and (14) with changing κ for $\Delta_{\mathrm{loc}}=1$ and $\Delta=0.1$ is shown in Fig. 3 (we suppose that the vector $\mathbf{k}$ is located at the Fermi surface (FS) and $\varepsilon_{\mathbf{k}+\mathbf{Q}}=0$ due to nesting). One can see that at small κ, i.e., in the vicinity of the Mott transition one finds splitting of Hubbard subbands, while the QP remains unsplit [Figs. 3(a) and 3(b)]. In the narrow region of larger κ the QP is split in two peaks, and the splitting of the Hubbard subbands remain visible [Fig. 3(c)]. At intermediate values of κ we find only splitting of the QP peak; the two other peaks corresponding to the Hubbard subbands are present [Figs. 3(d) and 3(e)]. Finally, in the weak-coupling limit $\kappa=1$ we reproduce the two-peak pseudogap, discussed in Refs. 12 and 15 [Fig. 3(f)]. In a more general case of $\gamma^{\nu,0}_{s,\mathbf{Q}}\neq 1$ we expect a pseudogap of the size $\sim\Delta(\gamma^{\Delta,0}_{s,\mathbf{Q}0})^{1/2}$ in the weak-coupling regime at small enough temperatures and more complicated structures at strong U; see our numerical results below.

V. MORIYAESQUE λ CORRECTION FOR THE VERTEX

The local approximation for the particle-hole irreducible vertex, considered in Sec. II, is however not exact. In particular, the magnetic transition temperature remains equal to its value in DMFT, and therefore it is overestimated in both three and two dimensions. In the latter case T_N would remain finite, contrary to the Mermin-Wagner theorem.

In the DΓA framework a reduction in T_N would naturally arise from a self-consistent solution of the DΓA equations. An alternative (simpler) way to fulfill the Mermin-Wagner theorem in 2D (and to reduce the transition temperature in three dimensions) is to introduce a correction to the susceptibility similar to the Moriya theory of weak itinerant magnets.[28] To this end, we replace

$$\chi^{s}_{\mathbf{q}\omega}\to[(\chi^{s}_{\mathbf{q}\omega})^{-1}+\lambda_{\mathbf{q}\omega}]^{-1}. \tag{15}$$

Formally the right-hand side (rhs) of Eq. (15) is exact for some (unknown) $\lambda_{\mathbf{q}\omega}$; in the following we assume $\lambda_{\mathbf{q}\omega}\simeq\lambda_{\mathbf{Q}0}\equiv\lambda$ since static fluctuations with momentum $\mathbf{Q}$ predominate near the magnetic instability. Instead of determining (as it was done in Moriya theory) λ from the fluctuation correction to the free energy, which is rather cumbersome in the present approach, we (similar to TPSC) impose the fulfillment of the sum rule

$$-\int_{-\infty}^{\infty}\frac{d\nu}{\pi}\mathrm{Im}\,\Sigma_{\mathbf{k},\nu}=U^2n(1-n/2)/2. \tag{16}$$

This also implies

$$\mathrm{Re}\,\Sigma_{\mathbf{k},\nu}\simeq\frac{U^2n(1-n/2)}{2\nu} \tag{17}$$

for $\nu\gg D$, according to the Kramers-Kronig relation. The latter asymptotic behavior may be very important to obtain the correct Fermi surface in the non-half-filled case, but should be fulfilled also in the half-filled case to obtain correct spectral functions. It is obviously violated in standard spin-fermion (also paramagnon) approaches in two dimensions, where the Néel temperature (T_N) is finite without the λ correction and the left-hand side (lhs) of Eqs. (16) and (17) are divergent at $T\to T_N$.

The frequency dependence of the self-energy at the imaginary axis for the two-dimensional Hubbard model ($U=D=4t$), calculated with and without λ correction, is compared in Fig. 4. The λ correction removes the divergence of the lhs of Eqs. (16) and (17) at $T\to T_N^{\mathrm{DMFT}}$ and leads to the correct asymptotic behavior at large ν_n. Without λ correction (or, alternatively, a self-consistent solution of the DΓA equations) spin fluctuations and their pertinent effect on the self-energy are overestimated. This is because the spin fluctuations result in a reduced metallicity which in a second DΓA iteration, i.e., the recalculation of the local vertex with the less metallic Green's function as an input,[32] would reduce the spin fluctuations.

In two dimensions sum rules (16) and (17) can be fulfilled at all positive temperatures, and the actual transition temperature is zero, as required by the Mermin-Wagner theorem. As one can see from Eqs. (12) and (13), the correlation length ξ in two dimensions is exponentially divergent (with λ correction),

$$\xi\propto\exp(b/T),$$

where the coefficient b in the exponent is proportional to U. This is evidently confirmed also by our numerical results shown in Fig. 5, where we have reported the values of the inverse of the spin susceptibility at $\mathbf{Q}=(\pi,\pi)$ calculated with the inclusion of the λ correction: The exponential divergence of ξ for $T\to 0$ is directly reflected in an analogous behavior

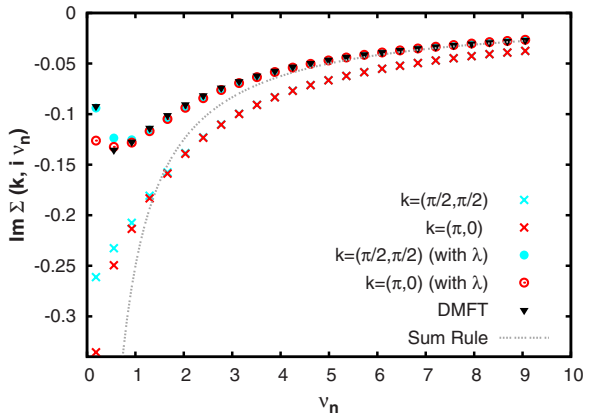

FIG. 4. (Color online) DΓA self-energy on the Matsubara axis calculated with and without Moriya λ correction for two different points of the Fermi surface in the two-dimensional Hubbard model (at $U=D=4t$ and $\beta=1/T=17$); also shown is the DMFT self-energy for comparison. Notice that, without introducing the Moriya λ correction, one always observes a deviation of the high-frequency $\Sigma(\mathbf{k},i\nu_n)$ from the correct asymptotic behavior $\sim U^2 n(1-\frac{n}{2})/(2i\nu_n)=U^2/(4i\nu_n)$ which is consistent with the self-energy sum rule (see text).

of the spin susceptibility [$\chi^s_{\mathbf{Q},0}\sim A\xi^2$, see Eq. (12)] at $T\to 0$.

In three dimensions, on the other hand, sum rules (16) and (17) with $(\chi^s_{\mathbf{Q},0})^{-1}+\lambda>0$ can be fulfilled only down to a certain temperature $T_N^{\mathrm{D\Gamma A}}$, which is reduced in comparison with T_N^{DMFT} and determines the phase transition temperature in the DΓA approach.

VI. RESULTS FOR THE HUBBARD MODEL IN THREE DIMENSIONS

Let us turn to the results for the self-energy and spectral functions which are obtained applying the Moriya λ correction to the vertex of the DΓA for the three-dimensional system (the analytical continuation to the real axis $i\nu_n\to\omega$ was

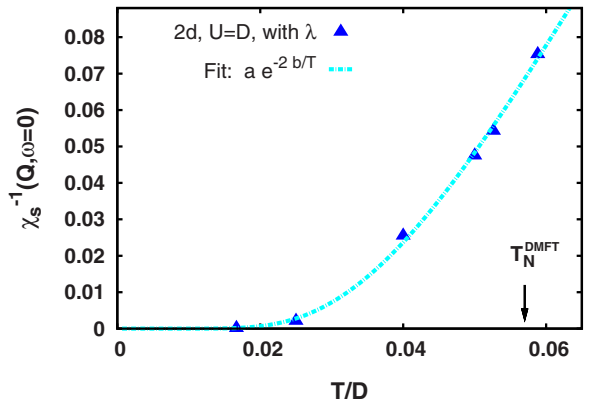

FIG. 5. (Color online) Temperature dependence of the λ-corrected inverse antiferromagnetic susceptibility in two dimensions (triangles) for $U=D=4t$. The data display an exponential temperature dependence, consistent with the expected behavior of ξ (see text). The DMFT Néel temperature corresponding to this set of parameters is marked with an arrow.

done using the Padé algorithm). In this case, as mentioned above, the λ correction is expected to result in small—and only quantitative—changes in the final DΓA results because in $d=3$ (where the antiferromagnetic long-range order survives at finite temperatures), the λ correction produces just a moderate reduction of the Néel temperature with respect to the DMFT value.

Our results, shown in Fig. 6, clearly confirm this expectation. Specifically, we analyze the case, already considered in our previous study Ref. 20, i.e., the three-dimensional Hubbard model with $U=1.5$ (in the units of half the variance of the noninteracting DOS, being $D\equiv 2\sqrt{6}t$ for $d=3$), and $\beta=11.2$ (in units of $1/D$), which corresponds to a temperature *slightly above* the DMFT Néel temperature (T_N^{DMFT}), but appreciably higher than the three-dimensional $T_N^{\mathrm{D\Gamma A}}$ with λ correction (an estimate of the λ-reduced Néel temperature gives $\beta^{\mathrm{D\Gamma A}}=1/T_N^{\mathrm{D\Gamma A}}\simeq 16.5$). In this situation, as noticed in Ref. 20 and shown in Fig. 6 (first row), the standard DΓA results display a sizable renormalization of the QP present in the DMFT spectrum. However, no qualitative change in the nature of the spectral functions can be observed. The inclusion of the Moriya λ correction, as shown in the second row of Fig. 6, reduces the renormalization effects due to nonlocal correlations: both the real and the imaginary parts of the DΓA self-energy at low frequency get very close to the DMFT values, and, obviously, the same happens to the QP peak in $A(\mathbf{k},\omega)$. This result is easily understood in terms of the reduction in T_N determined by the Moriya corrections since the enhanced distance to the second-order antiferromagnetic transition at T_N leads to a reduction in the spin-fluctuation and corrections to the DMFT self-energy. If we reduce the temperature toward the DΓA Néel temperature, antiferromagnetic spin fluctuations become strong again, and as shown in Fig. 7, we indeed find results which are qualitatively similar to those without λ correction (first row of Fig. 6). In particular, in both figures the quasiparticle weight is smaller in DΓA than in DMFT, in agreement with the expected effect of antiferromagnetic fluctuations.

Summing up the results for the isotropic three-dimensional system, we emphasize that the principal consequence of the inclusion of the Moriya λ correction is a shift of the region with appreciable nonlocal correlation effects (i.e., the region where the DΓA spectra substantially differ from DMFT) to lower temperatures, i.e., to the proximity of the "new" line of the antiferromagnetic phase transition. Our result demonstrates that for $d=3$—with or without lambda correction—the extension of the region characterized by relevant nonlocal correlations is relatively small even for intermediate values of the interactions. This indicates, hence, that for $d=3$ DMFT represents indeed a good approximation, except for the region close to the antiferromagnetic transition.

VII. RESULTS FOR THE HUBBARD MODEL IN TWO DIMENSIONS

The effects of nonlocal correlations are—as one can imagine—much more dramatic for a two-dimensional system. It is easy to figure out that the divergence of the ladder diagrams in the spin channel leads to huge nonlocal correc-

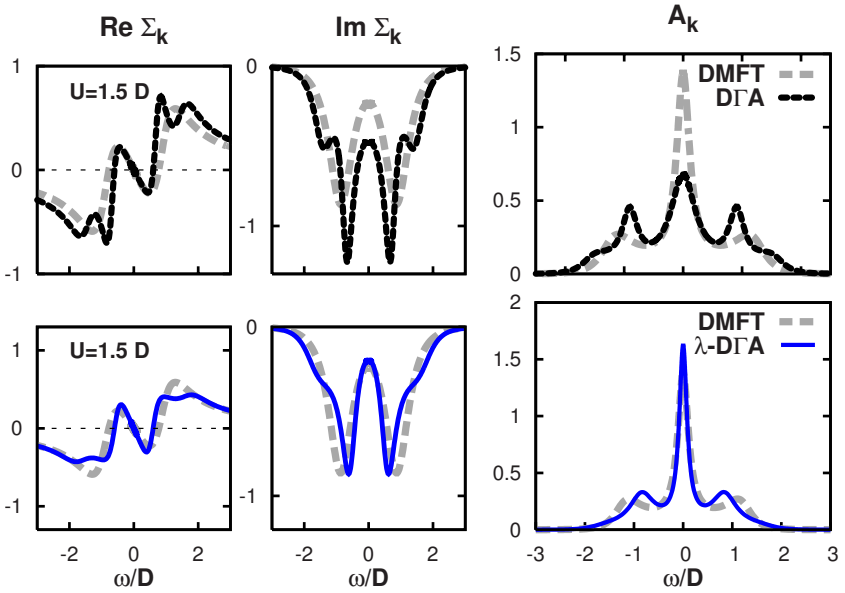

FIG. 6. (Color online) DMFT self-energies and spectral functions (gray dashed line) at $\mathbf{k}_F=(\pi/2,\pi/2,\pi/2)$ for the Hubbard model in $d=3$ at $U=1.5D$ ($D=2\sqrt{6}t$) and $\beta=11.2$ (i.e., slightly above T_N^{DMFT}) are compared with the corresponding DΓA results with (lower row; solid blue line) and without (upper row; black dotted line) Moriya λ correction. Note that (i) the nonlocal fluctuations modify only quantitatively the shape of the QP, but no pseudogap appears, and (ii) nonlocal correlation effects are further reduced by the inclusion of the Moriya λ correction.

tions in the DΓA self-energy, which can differ also qualitatively from the DMFT one. At the same time, one should expect that in two dimensions the nonlocal correlation effects could be sensibly overestimated by the DΓA without the inclusion of the Moriya λ correction. As we have discussed in Sec. V, these corrections are essential to fulfill the Mermin-Wagner theorem, pushing the Néel temperature from the DMFT value down to zero. Hence, for any finite temperature the antiferromagnetic fluctuations are reduced. The effects of the divergence of the spin ladder diagrams are also to some extent attenuated in the formula for the DΓA self-energy because of the extra dimension gained at $T=0$ due to the transformation of the Matsubara summation to a frequency integral on the rhs of Eq. (2).

In the light of these considerations, we can more easily interpret the results of the DΓA for the two-dimensional Hubbard model, which are presented in Figs. 8–10. Specifically, we start the analysis of the two-dimensional case, by evaluating the effects of the Moriya λ correction for the DΓA results computed for the half-filled Hubbard model with $U=4t$ at a temperature ($\beta=17$) *slightly above* the corresponding T_N in DMFT.

In the first/third row of Fig. 8, we show the DΓA self-energy and spectral function at the FS at the nodal $[\mathbf{q}=(\frac{\pi}{2},\frac{\pi}{2})]$ and antinodal $[\mathbf{q}=(\pi,0)]$ points computed without Moriya correction. One can clearly observe that, in contrast to the three-dimensional case, the DΓA spectra qualitatively differ from the original DMFT one because (i) a pseudogap appears at low frequencies and (ii) the spectra are markedly anisotropic in the nodal/antinodal direction, as the observed pseudogap is evidently more pronounced at the antinodal points.

As discussed above, the Moriya λ correction is however expected to be much more important in the two-dimensional than in the three-dimensional case. This is confirmed by the results shown in the second/fourth row of Fig. 8. In these panels the reduction in the nonlocal effects due to the inclusion of the Moriya λ correction in DΓA is evident. It is

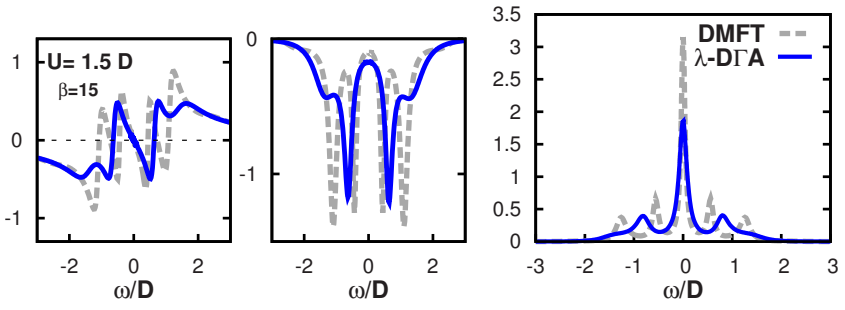

FIG. 7. (Color online) DMFT self-energies and spectral functions at $\mathbf{k}_F=(\pi/2,\pi/2,\pi/2)$ for the Hubbard model in $d=3$ at $U=1.5$ $D(D=2\sqrt{6}t)$ and $\beta=15$ compared with the corresponding DΓA ones with λ correction. Lowering $T=1/\beta$ toward $T_N^{\mathrm{DΓA}}$, qualitatively similar results as without λ correction at higher T (upper row of Fig. 6, $\beta=11.2$) are obtained.

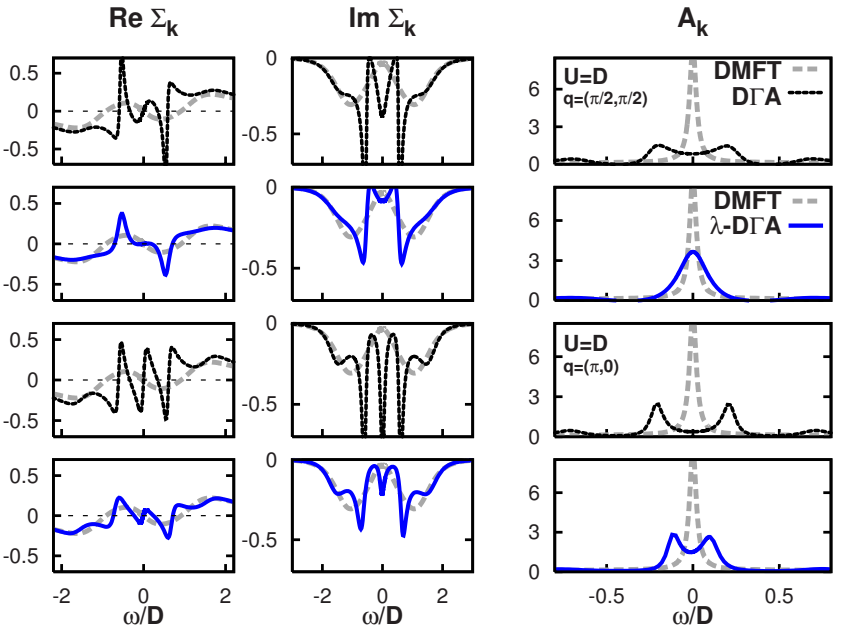

FIG. 8. (Color online) DΓA results for the half-filled two-dimensional Hubbard model at $U=D=4t$, $\beta=17$ (just slightly above T_N^{DMFT}) computed without (first and third row; black dotted line) and with (second and fourth row; blue solid line) the Moriya λ correction, and compared with DMFT (gray dashed line). The DΓA calculations in the non-self-consistent scheme show a clear pseudogap opening for the **k** points of the noninteracting FS, but more pronounced in the antinodal direction. Within the λ-corrected scheme, one can still notice a pseudogap opening but only in the antinodal direction, while in the nodal direction a strongly damped QP appears.

important noticing, however, that although the distance in the phase diagram from the actual antiferromagnetic transition (occurring at $T=0$ for $d=2$) is considerably larger than for $d=3$, nonlocal correlation effects are nonetheless extremely strong. Turning to the details, we still observe a remarkable anisotropy in the DΓA spectra after the inclusion of Moriya correction, with a strongly renormalized QP peak in the nodal direction and a rather clear pseudogap in the antinodal direction. The results of DΓA (implemented with the Moriya correction) indicate, hence, that for the two-dimensional system at half-filling antiferromagnetic fluctuation effects predominate in a wide region of the phase diagram, determining the onset of an anisotropic pseudogap in the spectra also for

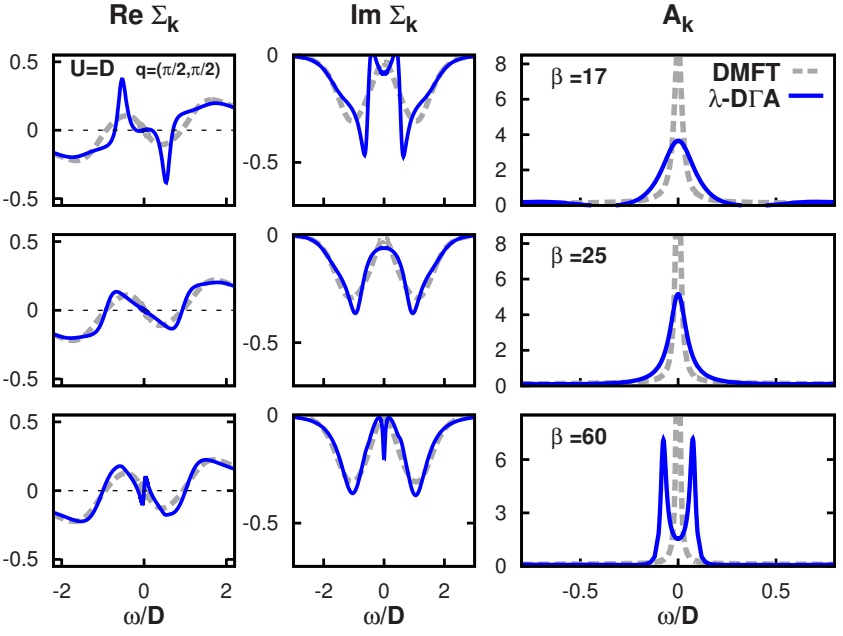

FIG. 9. (Color online) Temperature evolution of the DΓA results for the half-filled two-dimensional Hubbard model at $U=D=4t$ in the nodal direction, computed with the Moriya λ correction, and compared with DMFT. A clear pseudogap emerges at the lowest temperature ($\beta=60$), similarly to the results of the non-self-consistent scheme in the proximity of T_N^{DMFT} (see Fig. 8).

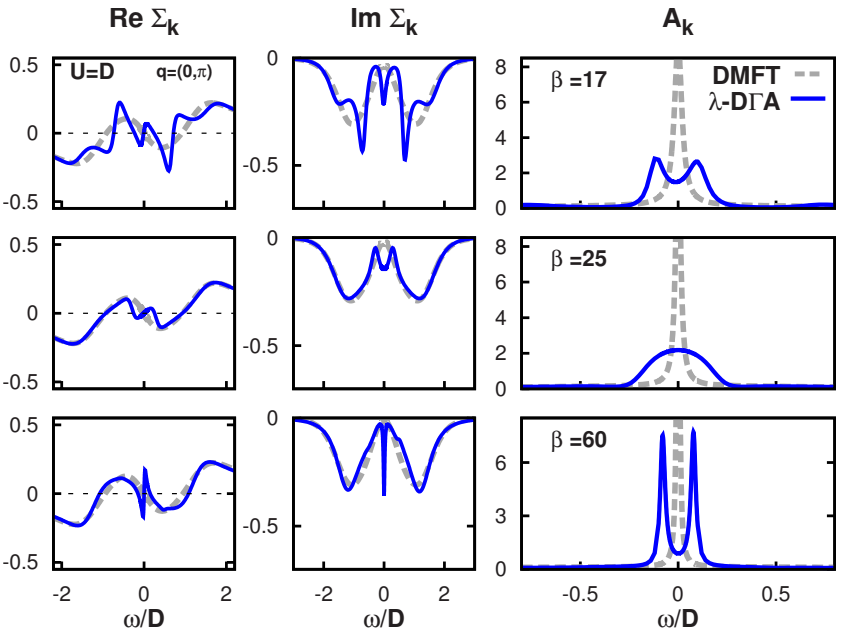

FIG. 10. (Color online) Same as in Fig. 9 in the antinodal direction. As expected, a very pronounced pseudogap characterizes the lowest temperature results. The behavior of the spectral functions is not completely monotonous, as the pseudogap seems to disappear at $\beta=25$. At all temperatures, however, the pseudogap features are always more marked in the antinodal than in the nodal direction.

considerably high temperatures, qualitatively similar to that observed in underdoped cuprates.[33]

The inclusion of the Moriya correction in DΓA allows us to extend our analysis to the low-temperature regime $T < T_N^{\mathrm{DMFT}}$. In particular, we are interested to study the evolution of the spectral function when the temperature is considerably reduced compared to the DMFT value T_N^{DMFT}. In Figs. 9 and 10 we report the DΓA calculation for the self-energy and the spectral function for the same case considered above ($U=4t$, half-filling) for three different decreasing temperatures ($\beta=17$, shown already in Fig. 8, $\beta=25$, and $\beta=60$) in the nodal and antinodal directions, respectively. First, we note that the anisotropy in the self-energy and the spectra remains visible at all temperatures. In addition, a marked tendency toward a completely gapped spectrum can be seen at the lowest temperature: At lowest temperature ($\beta=60$) a pseudogap appears also in the nodal direction, while the pseudogap already present in the antinodal direction becomes remarkably more profound. At this temperature, therefore, the anisotropy is reduced in comparison to the higher T cases—due to the strong depletion of spectral weight at $\omega=0$. This results can be understood in terms of the closer proximity to the antiferromagnetic instability at $T=0$, and is consistent with the marked pseudogap visible in the *k-integrated* spectral function obtained by means of cluster DMFT in Ref. 17.

It is worth noticing, however, that the temperature evolution toward the formation of a fully gapped spectrum at $T \to 0$ does not appear to be completely monotonous. The effects of the nonlocal fluctuations seem to be slightly weaker in the DΓA results for $\beta=25$ (second row in Figs. 9 and 10), than for $\beta=17$ (first row). More specifically, this is visible in the slightly *more Fermi-liquid-like* behavior of the real and imaginary part of the self-energies at $\beta=25$ in comparison to $\beta=17$.

A possible interpretation of this specific feature of our results is to relate the nonmonotonous temperature evolution in the DΓA spectral function to a competition between nonlocal and local mechanisms capable of destroying coherent excitations: (i) The (nonlocal) antiferromagnetic fluctuations, which become less pronounced with increasing T, making the system more metallic ($\chi^s_{\mathbf{Q},0}=8.9\times10^3$, 39.26, and 13.28, for $\beta=60$, 25, and 17, respectively); and at the same time (ii) the thermal loss of coherence, which is at the origin of so-called crossover region in the (purely local) DMFT and reflects increasing values of the quasiparticle damping [$\gamma=-\mathrm{Im}\,\Sigma(0)=0.009$, 0.021, and 0.034, for the three considered temperatures, respectively]. The relevance of the interplay between these two mechanisms is an interesting issue raised by our DΓA results. It might also be related to a similar nonmonotonous trend in the cluster DMFT phase diagram reported by Park *et al.*[34]

The DΓA results at stronger interaction ($U=2D$ and $\beta=40$) are presented in Fig. 11. At the considered low temperature the local DMFT spectral functions have peaky structure because we solve the impurity problem of DMFT by means of exact diagonalization (ED), which treats only finite number of sites. Note, however, the DΓA spectral functions are continuous due to momenta and frequency sums in Eq. (8), even though ED is employed as an impurity solver. The nonlocal spectral functions show the splitting of the quasiparticle peak due to magnetic correlations, which is similar to the structure (d) in Fig. 3 discussed in Sec. IV.[22] Closer to the Mott transition (i.e., at even stronger U) we also expect the formation of the structures (a)–(c) of Fig. 3.

The presented results demonstrate that the DΓA approach—with the inclusion of the Moriya corrections—allows for a nontrivial analysis of the effects of long-range spatial correlations in every region of the phase diagrams of strongly interacting fermionic systems both in two and three dimensions.

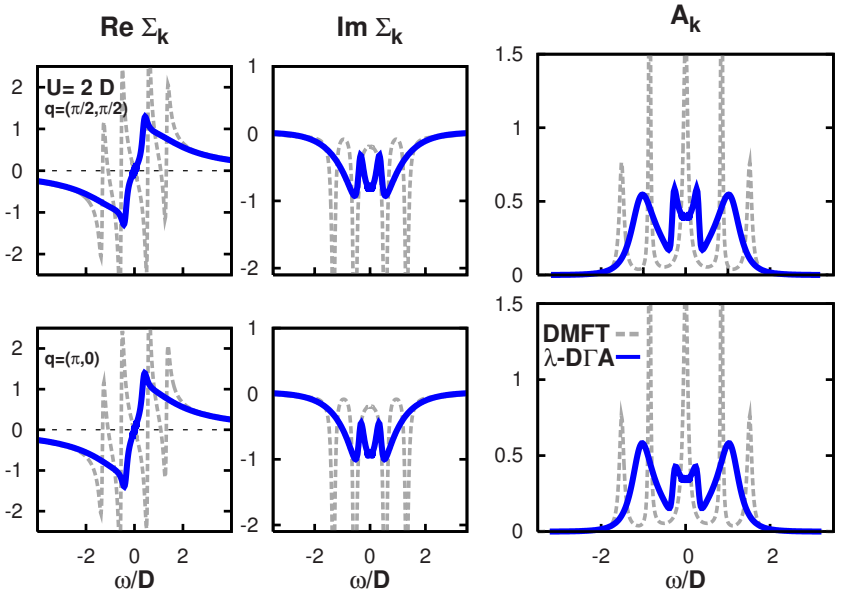

FIG. 11. (Color online) DΓA results with λ corrections for the half-filled two-dimensional Hubbard model at $U=2D=8t$, $\beta=40$ compared with the corresponding DMFT ones.

VIII. k-RESOLVED SPECTRAL FUNCTIONS IN TWO DIMENSIONS

Let us now calculate the **k** dependence of the spectral functions in the directions of high symmetry, as can be observed in angular resolved photoemission spectroscopy (ARPES). It is worthwhile remarking that, in contrast to the cluster extensions of DMFT, this does not require any kind of interpolation in **k** space: Due to the diagrammatic nature of the DΓA, the spectra for every chosen **k** point in the first Brillouin zone are easily computed via Eq. (2).

Here, in Fig. 12, we present DΓA results with Moriya λ correction for the same case previously considered in Fig. 8 (second and fourth row). As it is often done, we consider two different **k** paths along the Brillouin zone, the first one along the nodal direction $[(0,0)\rightarrow(\pi,\pi)$, left panel] and the second one right at the border of the Brillouin zone, crossing the antinodal point at the FS $[(\pi,\pi)\rightarrow(\pi,0)$, right panel].

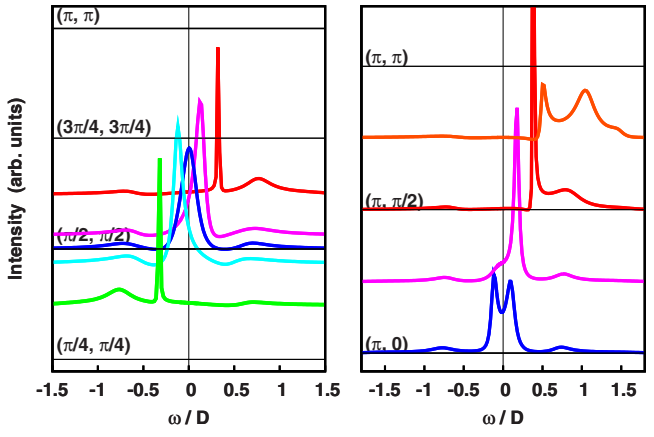

FIG. 12. (Color online) **k**-resolved DΓA spectra along the nodal (left) and antinodal (right) direction for the half-filled two-dimensional Hubbard model at $U=D=4t$ and $\beta=17$, calculated with the Moriya λ correction.

Our analysis of the **k**-resolved DΓA results allows us to appreciate the evolution of the main features of the DΓA spectral functions. Specifically, we observe that for the points most far away from the FS, the spectral functions display similar features in the two cases: A relatively narrow peak separated from a broader maximum at higher energies, which represents the incoherent processes building up the (upper) Hubbard band. When proceeding in the direction of the FS, as expected, the narrow peak moves toward the Fermi energy, while the broad feature becomes less pronounced. A qualitative difference between the two selected paths emerges only in the vicinity of the FS: The shift of the narrow peak down to zero energy is frozen along the second path, consistent with the opening of the anisotropic pseudogap in the antinodal direction, while it continues to shift down to the Fermi level in the nodal directions.

It is also worth noticing the occurrence in both cases of a slight broadening of the narrow peak while approaching the FS. This trend, which is markedly different from any FL expectation, could be understood in terms of the maximum of Im $\Sigma(\mathbf{k},\omega)$ appearing at zero frequency (see again Fig. 8) for both directions. The enhanced value of Im $\Sigma(\mathbf{k},\omega)$ at low frequencies, which is ultimately responsible for the opening of the pseudogap starting at the antinodal points, determines a loss of coherence and, hence, the observed broadening of the peak, while it moves closer to the FS.

IX. CONCLUSION

Based on the representation of the nonlocal self-energy which considers the effect of the bare Coulomb interaction and charge (spin) fluctuations, we have extended the recently introduced dynamical vertex approximation (DΓA) by including a Moriyaesque λ correction to the local vertex in Sec. V. The value of λ is determined from the sum rule which relates ω-integrated self-energy and occupation and

allows for a proper reduction in the DMFT Néel temperature, in two dimensions even to $T_N=0$ so that the Mermin-Wagner theorem is fulfilled. This correction is therefore particularly important for two dimensions, where spin fluctuations are especially strong. Without the Moriya λ correction, a much more involved self-consistent solution of the DΓA equations would be necessary to yield similar results.

The method we have introduced here allows for a treatment of nonlocal long-range spatial correlation in finite-dimensional systems. In three dimensions, pronounced effects of nonlocal spin fluctuations are found only close to the antiferromagnetic phase transition. This is in contrast to the two-dimensional case where antiferromagnetic fluctuations completely reshuffle the spectrum, also far away from the antiferromagnetic phase transition at $T_N=0$, leading eventually to the formation of a pseudogap. Qualitatively, the spectral functions can be understood by means of the analytical formula for the self-energy proposed in Sec. IV. Calculating several DΓA self-energies along the high-symmetry lines of the Brillouin zone, we obtain the momentum dependence of the spectral functions, which could be directly compared with the ARPES data.

DΓA can serve as a very promising method for future studies of the Hubbard model at noninteger filling, in particular in the vicinity of the antiferromagnetic quantum critical point.[30,35] A further important development would be also the generalization of the method to the multiorbital case, to analyze the effects of nonlocal correlations beyond DMFT in realistic band-structure calculations.[36]

ACKNOWLEDGMENTS

We thank W. Metzner, M. Capone, C. Castellani, G. Sangiovanni, and R. Arita for stimulating discussions and are indebted to M. Capone also for providing the DMFT(ED) code which has served as a starting point. This work has been supported by the EU-Indian cooperative network MONAMI. The work of A.K. was supported by the Russian Basic Research Foundation through Grants No. 1941.2008.2 (Support of Scientific Schools) and No. 07-02-01264a.

[1] J. Hubbard, Proc. R. Soc. London, Ser. A **276**, 238 (1963); M. C. Gutzwiller, Phys. Rev. Lett. **10**, 159 (1963); J. Kanamori, Prog. Theor. Phys. **30**, 275 (1963).
[2] E. H. Lieb and F. Y. Wu, Phys. Rev. Lett. **20**, 1445 (1968).
[3] W. Metzner and D. Vollhardt, Phys. Rev. Lett. **62**, 324 (1989).
[4] A. Georges and G. Kotliar, Phys. Rev. B **45**, 6479 (1992).
[5] A. Georges, G. Kotliar, W. Krauth, and M. Rozenberg, Rev. Mod. Phys. **68**, 13 (1996).
[6] R. Bulla, Phys. Rev. Lett. **83**, 136 (1999).
[7] N. F. Mott, Rev. Mod. Phys. **40**, 677 (1968); N. F. Mott, *Metal-Insulator Transitions* (Taylor & Francis, London, 1990); F. Gebhard, *The Mott Metal-Insulator Transition* (Springer, Berlin, 1997).
[8] M. Jarrell, Phys. Rev. Lett. **69**, 168 (1992).
[9] D. Vollhardt, N. Blümer, K. Held, M. Kollar, J. Schlipf, and M. Ulmke, Z. Phys. B: Condens. Matter **103**, 283 (1997).
[10] E. Dagotto, Rev. Mod. Phys. **66**, 763 (1994).
[11] N. E. Bickers, D. J. Scalapino, and S. R. White, Phys. Rev. Lett. **62**, 961 (1989).
[12] Y. M. Vilk and A.-M. S. Tremblay, J. Phys. I **7**, 1309 (1997).
[13] J. Polchinski, Nucl. Phys. B **231**, 269 (1984); D. Zanchi and H. J. Schulz, Phys. Rev. B **54**, 9509 (1996); **61**, 13609 (2000); C. J. Halboth and W. Metzner, *ibid.* **61**, 7364 (2000); C. Honerkamp, M. Salmhofer, N. Furukawa, and T. M. Rice, *ibid.* **63**, 035109 (2001); C. Honerkamp and M. Salmhofer, *ibid.* **64**, 184516 (2001).
[14] J. J. Deisz, D. W. Hess, and J. W. Serene, Phys. Rev. Lett. **76**, 1312 (1996); J. Altmann, W. Brenig, and A. P. Kampf, Eur. Phys. J. B **18**, 429 (2000).
[15] B. Kyung, Phys. Rev. B **58**, 16032 (1998); S. Moukouri, S. Allen, F. Lemay, B. Kyung, D. Poulin, Y. M. Vilk, and A.-M. S. Tremblay, *ibid.* **61**, 7887 (2000).
[16] D. Zanchi, Europhys. Lett. **55**, 376 (2001); C. Honerkamp and M. Salmhofer, Phys. Rev. B **67**, 174504 (2003); A. A. Katanin and A. P. Kampf, Phys. Rev. Lett. **93**, 106406 (2004); D. Rohe and W. Metzner, Phys. Rev. B **71**, 115116 (2005).
[17] M. H. Hettler, A. N. Tahvildar-Zadeh, M. Jarrell, T. Pruschke, and H. R. Krishnamurthy, Phys. Rev. B **58**, R7475 (1998); C. Huscroft, M. Jarrell, Th. Maier, S. Moukouri, and A. N. Tahvildarzadeh, Phys. Rev. Lett. **86**, 139 (2001); A. I. Lichtenstein and M. I. Katsnelson, Phys. Rev. B **62**, R9283 (2000); G. Kotliar, S. Y. Savrasov, G. Pálsson, and G. Biroli, Phys. Rev. Lett. **87**, 186401 (2001); T. A. Maier, M. Jarrell, T. Pruschke, and M. H. Hettler, Rev. Mod. Phys. **77**, 1027 (2005); E. Koch, G. Sangiovanni, and O. Gunnarsson, Phys. Rev. B **78**, 115102 (2008).
[18] A. Schiller and K. Ingersent, Phys. Rev. Lett. **75**, 113 (1995).
[19] V. Tokar and R. Monnier, arXiv:cond-mat/0702011 (unpublished).
[20] A. Toschi, A. A. Katanin, and K. Held, Phys. Rev. B **75**, 045118 (2007).
[21] Independently, a similar method, but with a cluster instead of a single-site as a starting point, was developed by C. Slezak, M. Jarrell, Th. Maier, and J. Deisz, arXiv:cond-mat/0603421 (unpublished).
[22] Similar, albeit less elaborated (complete), ideas were also independently developed by H. Kusunose, J. Phys. Soc. Jpn. **75**, 054713 (2006).
[23] Susceptibilities have been recently calculated also by G. Li, H. Lee, and H. Monien, Phys. Rev. B **78**, 195105 (2008).
[24] A. N. Rubtsov, M. I. Katsnelson, and A. I. Lichtenstein, Phys. Rev. B **77**, 033101 (2008); S. Brener, H. Hafermann, A. N. Rubtsov, M. I. Katsnelson, and A. I. Lichtenstein, *ibid.* **77**, 195105 (2008).
[25] E. Z. Kuchinskii, I. A. Nekrasov, and M. V. Sadovskii, JETP Lett. **82**, 198 (2005); M. V. Sadovskii, I. A. Nekrasov, E. Z. Kuchinskii, Th. Pruschke, and V. I. Anisimov, Phys. Rev. B **72**, 155105 (2005).
[26] J. A. Hertz and D. M. Edwards, J. Phys. F: Met. Phys. **3**, 2174 (1973).
[27] J. A. Hertz, Phys. Rev. B **14**, 1165 (1976).

[28] T. Moriya, *Spin Fluctuations in Itinerant Electron Magnetism* (Springer, New York, 1985).
[29] P. Monthoux, A. V. Balatsky, and D. Pines, Phys. Rev. Lett. **67**, 3448 (1991); Phys. Rev. B **46**, 14803 (1992).
[30] Ar. Abanov, A. V. Chubukov, and J. Schmalian, Adv. Phys. **52**, 119 (2003).
[31] K. Byczuk, R. Bulla, R. Claessen, and D. Vollhardt, Int. J. Mod. Phys. B **16**, 3759 (2002).
[32] For an elementary introduction, see K. Held, A. A. Katanin, and A. Toschi, Prog. Theor. Phys. Suppl. **176**, 117 (2008).
[33] For a review see, e.g., T. Timusk and B. W. Statt, Rep. Prog. Phys. **62**, 61 (1999) and A. Damascelli, Z. Hussain, and Z.-X. Shen, Rev. Mod. Phys. **75**, 473 (2003).
[34] H. Park, K. Haule, and G. Kotliar, Phys. Rev. Lett. **101**, 186403 (2008).
[35] S. Paschen, T. Lühmann, S. Wirth, P. Gegenwart, O. Trovarelli, C. Geibel, F. Steglich, P. Coleman, and Q. Si, Nature (London) **432**, 881 (2004); J. Custers, P. Gegenwart, H. Wilhelm, K. Neumaier, Y. Tokiwa, O. Trovarelli, C. Geibel, F. Steglich, C. Pepin, and P. Coleman, *ibid.* **424**, 524 (2003).
[36] V. I. Anisimov, A. I. Poteryaev, M. A. Korotin, A. O. Anokhin, and G. Kotliar, J. Phys.: Condens. Matter **9**, 7359 (1997); A. I. Lichtenstein and M. I. Katsnelson, Phys. Rev. B **57**, 6884 (1998); G. Kotliar, S. Y. Savrasov, K. Haule, V. S. Oudovenko, O. Parcollet, and C. A. Marianetti, Rev. Mod. Phys. **78**, 865 (2006); K. Held, Adv. Phys. **56**, 829 (2007).